Atomic layer deposition of Ru from CpRu(CO2)Et using O2 gas and O2 plasma

Atomic layer deposition of Ru from $CpRu(CO)_2Et$ using O_2 gas and O_2 plasma

N. Leick and R. O. F. Verkuijlen
Eindhoven University of Technology, P.O. Box 513, 5600 MB Eindhoven, The Netherlands

L. Lamagna
Laboratorio MDM, IMM-CNR, Via C. Olivetti, 2, 20041 Agrate Brianza (MB), Italy

E. Langereis
Eindhoven University of Technology, P.O. Box 513, 5600 MB Eindhoven, The Netherlands

S. Rushworth
SAFC Hitech Limited Power Road, Bromborough, Wirral CH62 3QF, United Kingdom

F. Roozeboom
Eindhoven University of Technology, P.O. Box 513, 5600 MB Eindhoven, The Netherlands and NXP-TSMC Research Center, High Tech Campus 4, 5656 AE Eindhoven, The Netherlands

M. C. M. van de Sanden and W. M. M. Kessels[a)]
Eindhoven University of Technology, P.O. Box 513, 5600 MB Eindhoven, The Netherlands

(Received 18 October 2010; accepted 24 January 2011; published 16 February 2011)

The metalorganic precursor cyclopentadienylethyl(dicarbonyl)ruthenium ($CpRu(CO)_2Et$) was used to develop an atomic layer deposition (ALD) process for ruthenium. O_2 gas and O_2 plasma were employed as reactants. For both processes, thermal and plasma-assisted ALD, a relatively high growth-per-cycle of ~1 Å was obtained. The Ru films were dense and polycrystalline, regardless of the reactant, yielding a resistivity of ~16 $\mu\Omega$ cm. The O_2 plasma not only enhanced the Ru nucleation on the TiN substrates but also led to an increased roughness compared to thermal ALD. © *2011 American Vacuum Society.* [DOI: 10.1116/1.3554691]

I. INTRODUCTION

High density metal-insulator-metal (MIM) capacitors are required for next generation dynamic random access memories with equivalent oxide thickness (EOT) values of 0.35 nm.[1,2] MIM capacitors integrated in silicon have also emerged as feasible candidates to reach the capacitance densities >500 nF/mm^2 required for automotive and decoupling applications. To meet the technical specifications, strontium titanate $SrTiO_3$ (STO) is currently one of the most investigated dielectric materials for these capacitor applications.[2] Crystalline STO has an ultrahigh dielectric constant [theoretically, $k \geq 300$ (Ref. 3)] at room temperature and amorphous films have a low crystallization temperature (T ~ 500–600 °C).[4] As electrode material in the MIM capacitors, noble metals, such as Pt and Ru,[5,6] are preferentially considered. In addition to a high work function, these metals have a sufficiently low resistivity such that ultrathin films can be employed. Moreover, these noble metals seem able to minimize the device's leakage current[7] and they appear to have a better chemical compatibility with STO compared to more conventional electrode materials such as TiN. Ru, having a bulk resistivity of 7.1 $\mu\Omega$ cm and a work function of 4.7 eV, is preferred from a device-integration perspective as it can be dry etched relatively easily, unlike platinum (Pt).[2,8] Ru is also chemically stable toward oxygen, forming a stable, conductive oxide.

The work described in this article focuses on atomic layer deposition (ALD) of Ru, which is a technique able to fulfill the requirements of the ultrathin films (thickness ~5 nm) and conformality for the high-aspect ratio structures to be employed (electrode conformality >70% for an aspect ratio of ~30).[9] For STO, the method has already shown promise to keep a low leakage current ($\sim 1 \times 10^{-8}$ A/cm^2) and a low EOT value (1.5 nm).[10] In the past years, numerous metalorganic precursors, such as $Ru(thd)_3$,[11] $Ru(acac)_3$,[12,13] $RuCp_2$,[12,14–17] and $Ru(EtCp)_2$,[17–19] have been used with O_2 gas for Ru ALD. Employing $RuCp_2$, Aaltonen *et al.*[20] showed that these processes rely on the ability of Ru to dissociatively chemisorb O_2, providing atomic O necessary for the oxidation of the precursor ligands. However, due to their relatively long nucleation delays [70–250 cycles (Refs. 14, 21, and 22)] and relatively low growth rates [0.2–0.8 Å/cycle (Refs. 12, 14, 17, 19, 23, and 24)], alternatives to the aforementioned ALD processes of Ru have been considered. To address these issues, the choice of both the Ru precursor and the co-reactant has been re-evaluated. For example, the nucleation delay has been successfully addressed using NH_3 plasmas,[17,19,24] which more easily initiated the Ru growth and delivered smooth films. However, the growth-per-cycle remained low [0.25–0.8 Å/cycle (Refs. 17, 19, and 24)] and NH_3 is also likely to chemically affect the STO during its integration in MIM capacitors.[25–28] Regarding Ru precursors, considerable attention has been devoted to new compounds, which have an improved reactivity and volatility. In light of this, several precursors, such as

a)Electronic mail: w.m.m.kessels@tue.nl

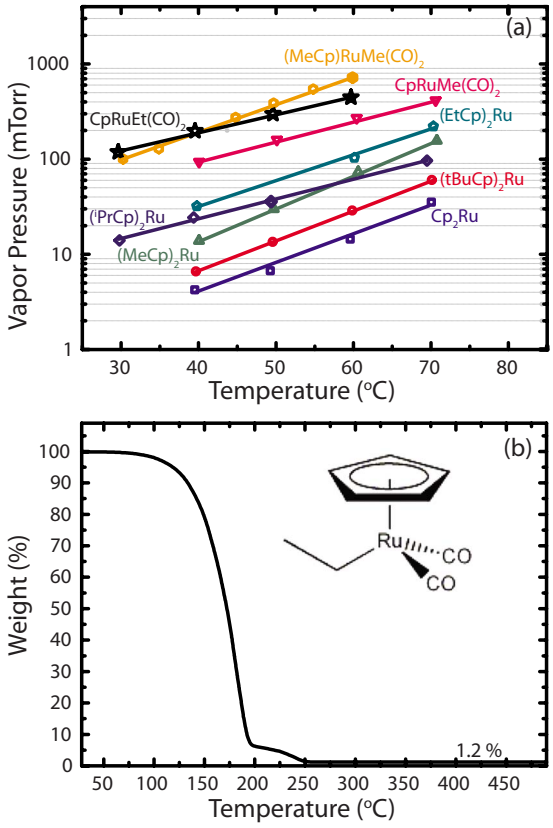

FIG. 1. (Color online) (a) Vapor pressure of cyclopentadienylethyl(dicarbonyl)ruthenium, compared with other metalorganic Ru precursors, and its (b) thermogravimetric analysis as a function of temperature. Inset: molecular structure of $CpRu(CO)_2Et$.

2,4-(dimethylpentadienyl)-(ethylcyclopentadienyl)ruthenium (DER),[21] RuO_4,[29] (η6-1-isopropyl-4-methyl-benzene)(η4-cyclohexa-1,3-diene)ruthenium ($C_{16}H_{22}Ru$),[30] 1-ethyl-1′-methyl-ruthenocene (EMR),[31] or bis(N,N'-di-tert-butylacetamidinato)ruthenium(II)dicarbonyl ($Ru(^tBu\text{-}Me\text{-}amd)_2(CO)_2$),[32] have become available for Ru ALD.

In this article, ALD of Ru was investigated using the recently developed precursor cyclopentadienylethyl(dicarbonyl)ruthenium ($CpRu(CO)_2Et$).[33] O_2 gas, as well as an O_2 plasma, was employed as the co-reactant. Providing O radicals directly from the gas phase, an O_2 plasma might facilitate nucleation of metals by ALD, as reported by Knoops *et al.*,[34] in the case of Pt. Moreover, an O_2 plasma is expected to be compatible with the STO, as mentioned before.

II. EXPERIMENT

$CpRu(CO)_2Et$ (SAFC Hitech®, purity > 99.999%) is a heteroleptic precursor that is liquid at room temperature, enhancing its evaporation over solid precursors. Figure 1(a) shows its high vapor pressure (0.4 Torr at 60 °C) compared to several other Ru precursors. Results from thermogravimetric analysis (TGA) in Fig. 1(b) show a first weight loss due to volatility and a feature at $T \sim 190$ °C due to decomposition. This could indicate the loss of the carbonyl groups since the same feature was observed for the related precursor $CpRu(CO)_2Me$. At higher temperatures (200–250 °C), a further weight loss took place, leading to a constant mass of 1.2%. During deposition, the precursor was heated to 90 °C and the precursor lines to 110 °C to prevent precursor condensation during transport to the deposition chamber. The precursor was vapor drawn into the reactor.

The Ru depositions were carried out in an Oxford Instruments FlexAL reactor,[35] consisting of a deposition chamber connected to a turbo pump (a base pressure of 10^{-6} Torr) and a remote inductively coupled plasma source allowing a maximum power of 500 W. The O_2 gas (purity > 99.999%) was delivered to the reactor through the plasma source, which was only switched on for the plasma-assisted ALD experiments. The pressure inside the deposition chamber was kept at 30 mTorr during each oxidant exposure. The temperature of the substrate carrier was 400 °C, which corresponds to a wafer temperature of ~325 °C, as deduced from calibration measurements.

The Ru films were deposited on Si wafers with native oxide, subsequently covered by an ~8 nm thick TiN film because Ru/TiN is expected to be a more feasible electrode stack than Ru only. The TiN film was deposited by plasma-assisted ALD in the same FlexAL reactor and at the same substrate temperature, using the process based on $TiCl_4$ and H_2–N_2 plasma developed by Knoops *et al.*[36]

The Ru film thickness and mass density were extracted from a Philips X'Pert MPD x-ray reflectometer (XRR) and the crystal structure from a grazing incidence x-ray diffractometer (GI-XRD). Rutherford backscattering spectroscopy (RBS) using a 2 MeV $^2He^+$ beam at the singletron facility of the Eindhoven University of Technology was employed to measure the areal densities of the Ru films. From the thickness values obtained by the XRR, the mass density of the films was also extracted from the RBS measurements. The sheet resistance of the Ru films was measured at room temperature by a four-point probe (FPP). Time-of-flight secondary ion mass spectrometry (ToF-SIMS) was performed by a dual beam ION-TOF IV instrument using Cs^+ ions of 1 keV for sputtering and Ga^+ ions of 25 keV for analysis. The roughness of the Ru films was investigated by atomic force microscopy (AFM) using a Veeco Dimension 3100 scanning probe microscope by scanning areas of 2×2 μm^2 on two different locations on each sample. The nucleation of the Ru films on TiN was studied by transmission electron microscopy (TEM) using the FEI Tecnai F30ST microscope operated at 300 kV. The measurements were performed on silicon nitride TEM membranes, on which an ~8 nm TiN layer was deposited by the same plasma-assisted ALD process as for the Si wafers.

III. RESULTS

Ru films were deposited for various numbers of cycles by thermal and plasma-assisted ALD. Figure 2 shows the results obtained from XRR, RBS, FPP, and AFM analysis as a function of the number of cycles. The unit cycle of the two ALD processes consisted of the following steps: $CpRu(CO)_2Et$ dose - Ar purge - O_2 dose - O_2 plasma excitation - Ar purge with the timings of 2-5-5-0-5 s for thermal ALD and 2-5-2-

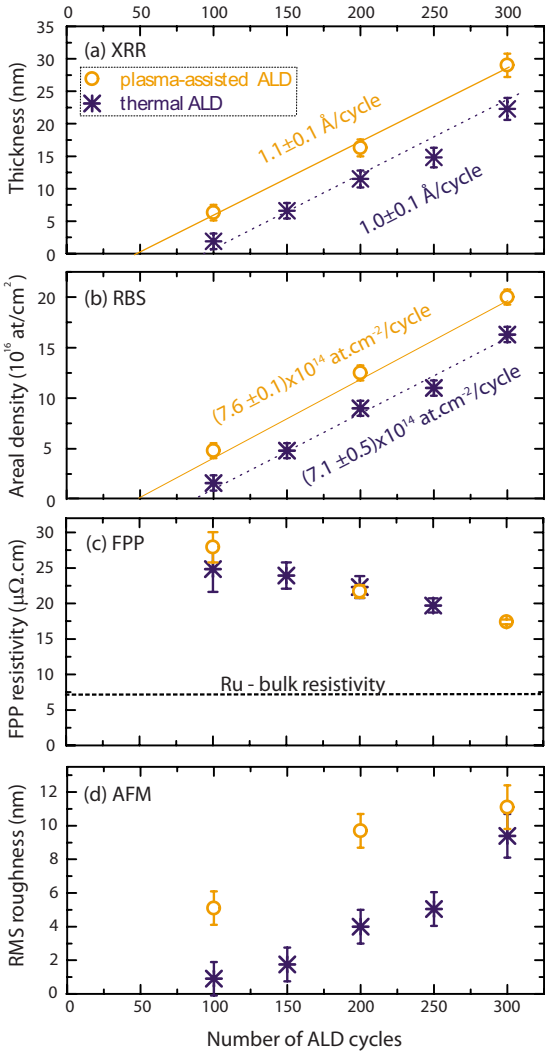

FIG. 2. (Color online) (a) Thickness determined by XRR as a function of the number of ALD cycles, (b) Ru areal density determined by RBS, (c) Ru resistivity measured by FPP, and (d) the rms roughness of the Ru films for plasma-assisted and thermal ALD. The growth-per-cycle in (a) (Å/cycle) and (b) ((at/cm^2 cycle) are given by the slope of the fitted lines and the nucleation delay by the extrapolation of the fits to zero thickness.

0.8-5 s for plasma-assisted ALD. For the plasma-based process, the O_2 dosing was inserted to stabilize the gas pressure in the reactor before igniting the plasma. The plasma exposure chosen was short (800 ms) to make sure that Ru was deposited, since for longer plasma exposures the films tended to become RuO_2. Furthermore, when operating the plasma source at relatively high powers, no film growth was observed. Therefore, a plasma power of 100 W was chosen. It is likely that at higher powers, the flux of reactive oxygen species is of such magnitude that etching of the Ru film[37] is dominating over deposition. This was also corroborated by a brief experiment in which Ru films were exposed to O_2 plasma and after few (<10 s) seconds, 0.3–0.5 nm had been etched off the films.

The aforementioned cycle timings resulted in saturated ALD conditions as verified by increasing the precursor dose time. We note that the substrate temperature (wafer temperature is ~325 °C) appears to be relatively high for the $CpRu(CO)_2Et$ precursor having carbonyl groups (see discussion about TGA in Sec. II). Our results showed, however, good agreement with the results obtained internally by SAFC Hitech and those recently reported by Park *et al.*,[33] and at lower temperatures, we observed reduced growth rates. At the wafer temperature of ~325 °C, also no growth occurred when only the precursor was dosed into the reactor without oxidant step. Moreover, for the ALD conditions, no sign of CVD-like growth was observed from film uniformity measurements (uniformity of thickness and sheet resistance <4% on 100 mm wafers for both plasma and thermal ALD). Investigations of the cracking pattern by quadrupole mass spectrometry did not reveal thermal decomposition products either. However, it still appears that the wafer temperature is such that the precursor is close to the onset of decomposition. Preliminary infrared studies, monitoring the initial reaction of the precursor on high surface area silica, revealed that the precursor starts decomposing at 325 °C.[33,38]

Figure 2(a) shows that the Ru thickness increase measured by XRR is linear with the number of cycles for both ALD processes. The growth-per-cycle has been determined from a linear fit to the data. Although within the experimental error, the growth-per-cycle of the plasma-based process of 1.1 Å seems to be slightly higher than the growth-per-cycle of 1.0 Å for thermal ALD. The latter is also confirmed by the RBS results in Fig. 2(b) from which the growth-per-cycle, in terms of Ru atoms deposited, can be determined. For thermal ALD, a value of $(7.1 \pm 0.5) \times 10^{14}$ at./cm^2 cycle can be deduced, whereas it is $(7.6 \pm 0.1) \times 10^{14}$ at./cm^2 cycle for plasma-assisted ALD. The slightly higher growth-per-cycle for the plasma-assisted process can possibly be attributed to the higher surface roughness of the films compared to those prepared by thermal ALD, as will be discussed below.

The Ru growth-per-cycle of ~1 Å for the $CpRu(CO)_2Et$ precursor is relatively high. Making the crude assumption of a Ru(0001) crystal structure (XRD results are discussed below), this growth rate corresponds roughly to ~0.5 ML/cycle. This is about twice as high as the growth obtained with other metalorganic precursors, such as $Ru(EtCp)_2$, DER, or EMR.[21,24,31] The growth-per-cycle is, however, quite similar to one of the new Ru ALD processes recently reported by Eom *et al.*[30] Using the open-ring compound $C_{16}H_{22}Ru$, a similarly high growth-per-cycle of 0.9 Å was obtained at 220 °C.

From XRR, the mass density of the films was determined, which suffered from a relatively large uncertainty (much more than the XRR thickness) due to a relatively large surface roughness, and values of 11 ± 1 g/cm^3 and 10 ± 1 g/cm^3 could be estimated for the thermal and plasma-assisted ALD films, respectively. From the combination of RBS results and thickness from XRR, more accurate values yielded a mass density of 12.2 ± 0.5 g/cm^3 for thermal ALD and 11.7 ± 0.5 g/cm^3 for plasma-assisted ALD. Despite the results obtained for both ALD processes being in agreement within the error, both measurement methods show a lower mass density for the films prepared by plasma-

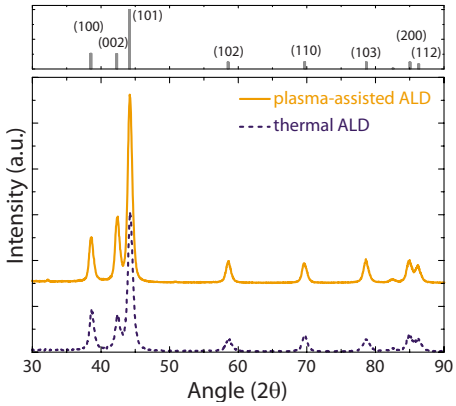

FIG. 3. (Color online) Grazing incidence XRD spectra of a 35 nm and of a 22 nm thick Ru film deposited by plasma-assisted and thermal ALD, respectively. The spectra are offset vertically for clarity. For comparison, the diffraction pattern of a Ru powder sample is also shown.

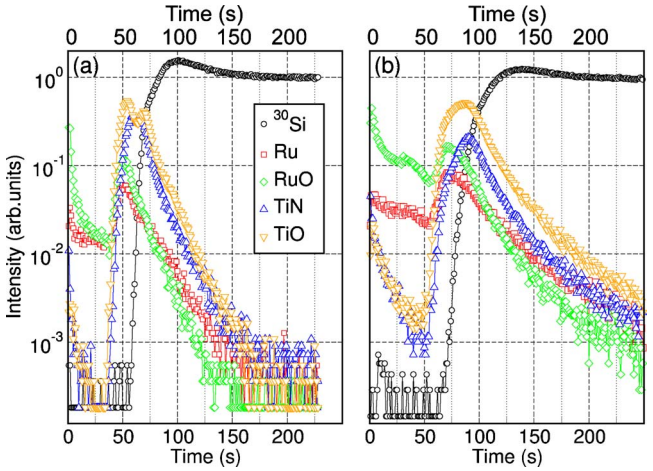

FIG. 4. (Color online) ToF-SIMS depth profiles of a 35 nm and of a 22 nm thick Ru film deposited by (a) plasma-assisted and (b) thermal ALDs, respectively.

assisted ALD. The difference might be explained by the presence of low levels of O in the films prepared by plasma-assisted ALD, as will be discussed below. The mass densities of the films are lower than the bulk density (12.4 g cm^{-3}) of Ru but within the same range of previously reported ALD films (8.7–12.0 g/cm^3).[23,24,31]

The resistivity of the films was calculated from the sheet resistance and the XRR thickness and is shown in Fig. 2(c) as a function of the ALD cycles. The resistivity decreased with thickness and the lowest value of 16 $\mu\Omega$ cm is reached for the thickest films (25–30 nm). This decrease is most likely related to the increasing grain size with thickness, decreasing the influence of grain boundary scattering. The resistivity is apparently independent of the oxidant and the value of 16 $\mu\Omega$ cm is in the range (12–35 $\mu\Omega$ cm) of other Ru films deposited by ALD.[12,14,15,18,19] Moreover, 5 nm Ru films reach a resistivity <30 $\mu\Omega$ cm, fulfilling the resistivity specifications (<300 $\mu\Omega$ cm for 5 nm) imposed on MIM capacitor electrodes.[9]

Figure 3 shows the GI-XRD θ-2θ scans of Ru films prepared by 300 cycles of thermal and plasma-assisted ALD. For the films prepared by both ALD methods, several diffraction peaks are observed from which it can be concluded that the films are polycrystalline with a hexagonal closed packed structure. The peaks for the plasma-assisted ALD Ru film have a higher intensity due to the higher thickness of that film. Similar polycrystalline films have been obtained by several other Ru ALD processes using metalorganic precursors and O_2 gas.[12,31,39] Since the relative peak intensities resemble those of the reference spectrum of a powder sample the crystallites in the Ru layer have no dominant crystallographic orientation, although it cannot be excluded that the film prepared by plasma-assisted ALD might be slightly preferentially oriented in the (002) and (101) planes. In a comparison between Ru ALD with O_2 gas and NH_3 plasma, Kwon *et al.*[24] also observed a (002) preferential orientation when a NH_3 plasma was used. The (002) orientation allows a more compact configuration of the Ru atoms than the other orientations and it is therefore possible that the crystallographic arrangement of the Ru atoms is influenced by additional energy delivered to the substrate by the plasma. The peak positions are the same for both samples, indicating no difference in lattice constants, which could be caused by differences in stress or composition. Furthermore, the peak widths of the plasma-assisted ALD film are slightly narrower than those of the thermal ALD film, indicating a slightly larger crystallite size or smaller crystal defect concentration for the film prepared by plasma-assisted ALD. This can possibly again be attributed to the higher energy flux to the substrate during the plasma exposure.

For both thermal and plasma-assisted ALD, the XRD spectra only revealed crystalline peaks related to Ru and no peaks from RuO_2 could be identified, in contrast to Park *et al.* who used the same precursor.[33] The presence of O in the films was examined by ToF-SIMS. As shown in Fig. 4 for the plasma-assisted ALD film, the RuO^+ signal is more pronounced than for thermal ALD. Moreover, TiO^+ is detected throughout the TiN film, as opposed to thermal ALD for which TiO^+ is predominantly detected at the Ru/TiN and TiN/SiO_2 interfaces. Although no evidence for RuO_2 was provided by XRD and RBS (within its rather high detection limit of $<20\%$ for O), more oxygen was detected by ToF-SIMS in the films deposited by the O_2 plasma, which is a stronger oxidant. This higher oxygen content is also a likely explanation for the slightly lower mass density of the Ru films deposited by plasma ALD.

XPS results on the thermal ALD film corroborated that the Ru was in the metallic state with only a small amount of oxygen present at the top surface of the film. The TiN was oxidized at the Ru interface but this could be caused by the oxidant step during ALD as well as by oxidation of the TiN when the film was exposed to ambient air after the TiN deposition. By XPS, only adventitious carbon at the top surface was detected, i.e., no significant amount of C in the film could be observed.

The Ru film properties discussed so far were quite similar for thermal and plasma-assisted ALD. However, larger dif-

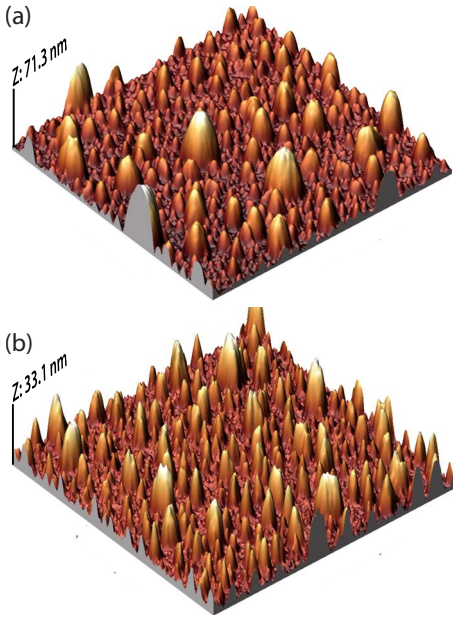

FIG. 5. (Color online) AFM scans for plasma-assisted and thermal ALD Ru films with thicknesses of (a) 16.3 nm and (b) 14.8 nm, respectively. Note the difference in height scale.

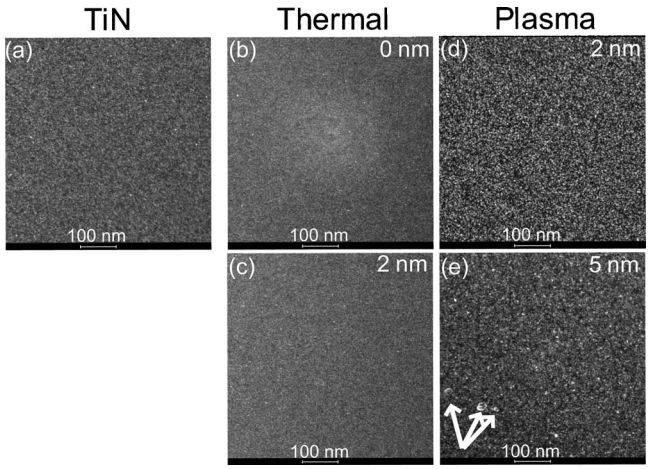

FIG. 6. TEM images of (a) a TiN-covered membrane, and of such membranes on which 50 and 100 cycles thermal [(b) and (c)] and plasma-assisted ALD [(d) and (e)] of Ru were carried out. The estimated thickness of the Ru layer is indicated in the images. The arrows indicate large Ru grains in (e).

ferences were observed in terms of film nucleation and surface roughness. As shown in Figs. 2(a) and 2(b), the O_2 plasma leads to faster nucleation of the Ru film than thermal ALD. Extrapolating the thickness and areal density data reveals that film nucleation takes place after ~45 cycles for plasma-assisted ALD, whereas it is delayed to ~85 cycles for thermal ALD. As mentioned in the Introduction (Sec. I), faster nucleation compared to thermal ALD was observed earlier for Ru films deposited by plasma-assisted ALD using a NH_3 plasma as the co-reactant.[17] Also in a comparison between O_2 gas and O_2 plasma as oxidants for ALD of Pt, a much faster nucleation was observed for the plasma-based process.[34] The higher reactivity of the plasma, providing reactive oxygen atoms from the gas phase, apparently promotes the nucleation of the Ru, potentially also through oxidation of the TiN surface forming TiO_2-like surface species.[5] However, as opposed to plasma-assisted ALD of Pt, no instant nucleation is observed. This could possibly be related to the fact that Ru can be etched by the O_2 plasma unlike Pt. This etching of Ru atoms can compete with the initial growth.

Considering the surface roughness of the films [Fig. 2(d)], it becomes clear that the Ru films deposited by plasma-assisted ALD have a significantly higher roughness than the films prepared by thermal ALD. Moreover, all Ru films are relatively rough and the roughness increased considerably with the number of ALD cycles. The AFM scan data, shown in Fig. 5 for two almost equivalently thick samples (14.8 and 16.3 nm for thermal and plasma-assisted ALDs, respectively), reveal a surface morphology consisting of densely packed Ru grains. When O_2 gas was used, the grains observed in the AFM scan have similar heights whereas the film deposited using an O_2 plasma consists of several dominant grains having different heights and which are randomly distributed over the surface. The root-mean-square (rms) roughness values of these ALD films, 5 and 9.6 nm for the thermal and plasma-assisted ALD films, respectively, are very high for ALD films compared to the surface roughness values reported so far. For thermal ALD of Ru, rms surface roughness values are typically within the range of 0.3–3.8 nm (for film thicknesses ranging from 5 to 80 nm),[18,31,32,40] while for plasma-assisted ALD films even values as low as 0.7 nm have been reported for 50 nm thick films.[24]

The results from the TEM measurements on the TiN-covered membranes are shown in Fig. 6. On these membranes, 50 and 100 cycles of thermal and plasma-assisted ALD were carried out. Due to the polycrystalline nature of the 8 nm thick TiN layer, the contrast is poor and no clear differences can be observed for the two depositions with thermal ALD. However differences with the TiN-covered membrane and the thermal ALD results are clearer for the plasma-assisted ALD experiments after 50 and 100 cycles. Already after 50 cycles of plasma-assisted ALD, a grain structure can be observed and after 100 cycles, it is clear that several large grains are present. The TEM images corroborate therefore the thickness and AFM results in that the nucleation of the plasma-assisted ALD films is enhanced and that the roughness increases with thickness through the development of large grains.

The high surface roughness could limit the applicability of the Ru films prepared from these processes, and especially electrode layers in MIM capacitors might require smooth films. Several factors can affect the surface roughness, including poor nucleation, modification and etching of the substrate and/or film, and precursor decomposition. However, based on the results reported, the high surface roughness can mainly be attributed to the combination of a relatively high substrate temperature and use of O_2 (plasma) as co-reactant.[12,18,31,32] For example, Kukli *et al.* reported high

roughness values (1.7 nm for a 5 nm thin film) for Ru prepared from EMR and O_2 at high substrate temperatures ($T \sim 400$ °C),[31] and Park *et al.*[33] reported a surface roughness of 1.4 nm for a film of only ~3.1 nm thickness prepared from $CpRu(CO)_2Et$ and O_2 at 300 °C. Using a ruthenium amidanate precursor and O_2, Wang *et al.*[32] found that the surface roughness and grain size increase with longer O_2 gas exposures (with a maximum roughness of ~2.5 nm for an ~30 nm thick film) with the grain size distribution becoming also non-uniform. Furthermore, Kwon *et al.*[18] carried out an experiment in which smooth Ru films (3.82 nm roughness for 80 nm film thickness) prepared by ALD at 270 °C were annealed at 600 and 750 °C in O_2. They observed a clear surface roughening resulting in surface roughnesses of 27.3 and 42.3 nm at 600 and 750 °C, respectively. On the other hand, annealing the same film at 750 °C in Ar barely affected the surface roughness (3.94 nm).

It is also interesting that the length of the nucleation period of our films prepared by the O_2 plasma-based ALD process is reduced, whereas the island-like growth is more pronounced. Generally a short nucleation delay and a low surface roughness of films prepared by ALD indicate a uniform film growth, whereas an enhanced film roughness and pronounced nucleation delay are characteristics for island-like growth.[5,17,41,42] This correlation was also observed for the Ru films deposited with a NH_3 plasma.[17] The situation in the present case appears therefore to be more complex and it is possible that several phenomena play a role simultaneously. A mechanism that could potentially also play a role is Ostwald ripening.[43,44] This mechanism could possibly explain the TEM and AFM data, suggesting that the nucleation sites can develop faster for plasma-assisted ALD and that grains become larger at the expense of smaller grains. Ostwald ripening is known to be enhanced by higher energy fluxes[45,46] and the energy flux during plasma-assisted ALD is certainly higher than for thermal ALD. Besides the flux of (reactive) oxygen atoms, the O_2 plasma contains also ions, which deliver energy to the substrate [under the conditions used the ion energy is ~10 eV and the ion flux is $\sim 10^{13}$ cm^{-2} s^{-1} (Ref. 47)]. This higher energy flux can increase the surface roughness and crystalline grain size for the plasma-assisted ALD films as discussed earlier (see also XRD results). More research is, however, necessary to draw conclusions about the mechanisms governing the nucleation delay and roughness development of the Ru films.

IV. CONCLUSIONS

Thermal and plasma-assisted ALD using O_2 and $CpRu(CO)_2Et$ both resulted in Ru films with properties that are similar to a large extent. The Ru films obtained were dense, polycrystalline with a hexagonal closed packed crystal structure, and had a low resistivity (16 $\mu\Omega$ cm). The thermal and plasma-assisted ALD processes also have a relatively high growth (1 Å/cycle), which is a main merit of both new processes. These properties make the ALD processes fit the requirements for the use of the Ru films as electrode layers in MIM capacitors. However, a major drawback for this application is the high surface roughness of the Ru films.

The O_2 plasma-based process showed a reduction of the nucleation delay down to ~45 ALD cycles; however, the plasma-assisted ALD Ru films showed also a higher surface roughness than the thermal ALD films. Therefore, from the combination of the film properties, no major benefits have emerged for the plasma-assisted ALD process of Ru over the thermal process under the operating conditions studied. The use of an O_2 plasma might be beneficial over thermal ALD at lower substrate temperatures. This needs, however, to be addressed in future work.

ACKNOWLEDGMENTS

Dr. P. C. J. Graat, R. Beerends (Philips MiPlaza Materials Analysis), and Dr. M. A. Verheijen (Eindhoven University of Technology) are thanked for carrying out the XRR, XRD, RBS, AFM, and TEM measurements, and M. Perego and C. Wiemer (MDM) are thanked for the ToF-SIMS analysis. C. van Helvoirt and W. Keuning are acknowledged for their technical support throughout this study. This work is funded by the Dutch Technology Foundation STW and is carried out in cooperation with the MaxCaps project (2T210) within the European Medea+ framework.

[1] ITRS, www.itrs.net.
[2] J. A. Kittl *et al.*, Microelectron. Eng. **86**, 1789 (2009).
[3] S. Van Elshocht *et al.*, J. Vac. Sci. Technol. B **27**, 209 (2009).
[4] M. Popovici *et al.*, J. Electrochem. Soc. **157**, G1 (2010).
[5] S. Y. Kang, C. S. Hwang, and H. J. Kim, J. Electrochem. Soc. **152**, C15 (2005).
[6] Y. Matsui, M. Hiratani, T. Nabatame, Y. Shimamoto, and S. Kimura, Electrochem. Solid-State Lett. **4**, C9 (2001).
[7] C. Vallée, P. Gonon, C. Jorel, F. El Kamel, M. Mougenot, and V. Jousseaume, Microelectron. Eng. **86**, 1774 (2009).
[8] T. Yunogami and T. Kumihashi, Jpn. J. Appl. Phys., Part 1 **37**, 6934 (1998).
[9] MaxCaps Consortium, Project No. 2T210.
[10] N. Menou *et al.*, J. Appl. Phys. **106**, 094101 (2009).
[11] T. Aaltonen, M. Ritala, K. Arstila, J. Keinonen, and M. Leskela, Chem. Vap. Deposition **10**, 215 (2004).
[12] T. Aaltonen, M. Ritala, Y. L. Tung, Y. Chi, K. Arstila, K. Meinander, and M. Leskela, J. Mater. Res. **19**, 3353 (2004).
[13] I. K. Igumenov, P. P. Sernyannikov, S. V. Trubin, N. B. Morozova, N. V. Gelfond, A. V. Mischenko, and J. A. Norman, Surf. Coat. Technol. **201**, 9003 (2007).
[14] T. Aaltonen, P. Alen, M. Ritala, and M. Leskela, Chem. Vap. Deposition **9**, 45 (2003).
[15] K. J. Park, J. M. Doub, T. Gougousi, and G. N. Parsons, Appl. Phys. Lett. **86**, 051903 (2005).
[16] S. J. Park, W. H. Kim, W. J. Maeng, Y. S. Yang, C. G. Park, H. Kim, K. N. Lee, S. W. Jung, and W. K. Seong, Thin Solid Films **516**, 7345 (2008).
[17] S. J. Park, W. H. Kim, H. B. R. Lee, W. J. Maeng, and H. Kim, Microelectron. Eng. **85**, 39 (2008).
[18] S. H. Kwon, O. K. Kwon, J. H. Kim, S. J. Jeong, S. W. Kim, and S. W. Kang, J. Electrochem. Soc. **154**, H773 (2007).
[19] S. S. Yim, M. S. Lee, K. S. Kim, and K. B. Kim, Appl. Phys. Lett. **89**, 093115 (2006).
[20] T. Aaltonen, A. Rahtu, M. Ritala, and M. Leskela, Electrochem. Solid-State Lett. **6**, C130 (2003).
[21] S. K. Kim, S. Y. Lee, S. W. Lee, G. W. Hwang, C. S. Hwang, J. W. Lee, and J. Jeong, J. Electrochem. Soc. **154**, D95 (2007).
[22] S. K. Kim, S. Hoffmann-Eifert, and R. Waser, J. Phys. Chem. C **113**, 11329 (2009).

[23]J. Choi *et al.*, Jpn. J. Appl. Phys. **41**, 6852 (2002).
[24]O. K. Kwon, S. H. Kwon, H. S. Park, and S. W. Kang, Electrochem. Solid-State Lett. **7**, C46 (2004).
[25]I. Marozau *et al.*, Appl. Surf. Sci. **255**, 5252 (2009).
[26]A. Shkabko, M. H. Aguirre, I. Marozau, T. Lippert, Y. H. Chou, R. E. Douthwaite, and A. Weidenkaff, J. Phys. D: Appl. Phys. **42**, 145202 (2009).
[27]A. Shkabko, M. H. Aguirre, I. Marozau, M. Doebeli, M. Mallepell, T. Lippert, and A. Weidenkaff, Mater. Chem. Phys. **115**, 86 (2009).
[28]J. J. Chambers, B. W. Busch, W. H. Schulte, T. Gustafsson, E. Garfunkel, S. Wang, D. M. Maher, T. M. Klein, and G. N. Parsons, Appl. Surf. Sci. **181**, 78 (2001).
[29]J. Gatineau, K. Yanagita, and C. Dussarrat, Microelectron. Eng. **83**, 2248 (2006).
[30]T. K. Eom, W. Sari, K. J. Choi, W. C. Shin, J. H. Kim, D. J. Lee, K. B. Kim, H. Sohn, and S. H. Kim, Electrochem. Solid-State Lett. **12**, D85 (2009).
[31]K. Kukli, M. Ritala, M. Kemell, and M. Leskela, J. Electrochem. Soc. **157**, D35 (2010).
[32]H. T. Wang, R. G. Gordon, R. Alvis, and R. M. Ulfig, Chem. Vap. Deposition **15**, 53 (2009).
[33]S. K. Park, R. Kanjolia, J. Anthis, R. Odedra, N. Boag, L. Wielunski, and Y. J. Chabal, Chem. Mater. **22**, 4867 (2010).
[34]H. C. M. Knoops, A. J. M. Mackus, M. E. Donders, M. C. M. van de Sanden, P. H. L. Notten, and W. M. M. Kessels, Electrochem. Solid-State Lett. **12**, G34 (2009).
[35]J. L. van Hemmen, S. B. S. Heil, J. H. Klootwijk, F. Roozeboom, C. J. Hodson, M. C. M. van de Sanden, and W. M. M. Kessels, J. Electrochem. Soc. **154**, G165 (2007).
[36]H. C. M. Knoops, L. Baggetto, E. Langereis, M. C. M. van de Sanden, J. H. Klootwijk, F. Roozeboom, R. A. H. Niessen, P. H. L. Notten, and W. M. M. Kessels, J. Electrochem. Soc. **155**, G287 (2008).
[37]D. Shamiryan, M. R. Baklanov, and W. Boullart, Electrochem. Solid-State Lett. **8**, G176 (2005).
[38]S. Haukka (personal communication).
[39]K. Frohlich *et al.*, Mater. Sci. Eng., B **109**, 117 (2004).
[40]K. Kukli *et al.*, J. Cryst. Growth **312**, 2025 (2010).
[41]S. M. George, Chem. Rev. **110**, 111 (2010).
[42]R. L. Puurunen and W. Vandervorst, J. Appl. Phys. **96**, 7686 (2004).
[43]D. A. Grigor'ev and S. A. Kukushkin, Tech. Phys. **43**, 846 (1998).
[44]A. Lo and R. T. Skodje, J. Chem. Phys. **112**, 1966 (2000).
[45]P. Berdahl, R. P. Reade, and R. E. Russo, J. Appl. Phys. **97**, 103511 (2005).
[46]S. Lucas and P. Moskovkin, Thin Solid Films **518**, 5355 (2010).
[47]H. B. Profijt, P. Kudlacek, M. C. M. van de Sanden, and W. M. M. Kessels (submitted).